

Research Article

Permeability, Compressibility and Pressure Prediction in Supercharged Wireline and FTWD EnvironmentsXiaofei Qin ¹, Yongren Feng ¹, Lejun Wu ¹, Zhongjian Tan ¹, Yanmin Zhou ¹, Wilson Chin ^{2, *}

1. China Oilfield Services Limited (COSL), Beijing, China; E-Mails: qinx@cosl.com.cn; fengyr@cosl.com.cn; wulj12@cosl.com.cn; tanzhj@offshoreoil.com.cn; zhouym3@cosl.com.cn
2. Stratamagnetic Software, LLC, Houston, Texas, USA; E-Mail: stratamagnetic.software@outlook.com

* **Correspondence:** Wilson Chin; E-Mail: stratamagnetic.software@outlook.com**Academic Editor:** Müslüm Arıcı

Journal of Energy and Power Technology
2023, volume 5, issue 3
doi:10.21926/jept.2303023

Received: April 12, 2023
Accepted: July 03, 2023
Published: July 10, 2023

Abstract

In conventional wireline and LWD/MWD formation testing, downhole predictions for rock and fluid properties are based on simplified Darcy flow models, but only for mathematical expediency. These require initially constant pressures that are uniform throughout the reservoir. This limitation precludes common applications in overbalanced drilling, so that supercharge or near-well invasion effects - associated with rapidly decreasing pressures at the sandface where pressures are measured - are completely ignored. Such 1990s math models are commonly used despite documented field results for overbalances as high as 2,000 psi. Incorrect modeling can produce incorrect predictions, leading to misleading formation evaluation results and economic analyses. Here, the conventionally accepted model (developed by the last author over two decades ago) is rigorously extended to allow general supercharge and also underbalanced drilling effects. The formulation and algorithm are explained and detailed pressure examples are offered showing essential differences between earlier and newer algorithms.

Keywords

Formation testing; invasion; supercharge; pressure transient analysis



© 2023 by the author. This is an open access article distributed under the conditions of the [Creative Commons by Attribution License](https://creativecommons.org/licenses/by/4.0/), which permits unrestricted use, distribution, and reproduction in any medium or format, provided the original work is correctly cited.

1. Introduction

1.1 Drilling and Well Logging Background

The formation tester is a borehole measurement tool having solid sealing pads that, when pushed against the porous face of the borehole, withdraws (or injects) liquids from (or into) the rock using a retractable piston. Samples are delivered to laboratories for detailed chemical analysis. Importantly, pressure transients during pumping are monitored, and rock and liquid attributes like permeability, anisotropy, compressibility, porosity and background pore pressure can be obtained from “drawdown,” “buildup” or “drawdown-buildup” pressure tests and special interpretation methods.

In conventional wireline and LWD/MWD formation testing, both post-logging and real-time predictions for underground attributes like permeability, anisotropy, compressibility, porosity and pore pressure are based on simplified Darcy flow models, again only for mathematical expediency. These require initially constant pressures that are uniform throughout the reservoir, a seemingly innocuous condition often invoked in pressure transient analysis. Unfortunately, this limiting assumption precludes applications to practical “overbalanced drilling,” so that supercharge effects and near-well invasion, which create rapidly varying spatial gradients with decreasing pressures near the sandface where pressure data are taken for inverse models, are completely ignored.

This restriction to uniform initial pressure also implies that problems in “underbalanced drilling” cannot be modeled, that is, situations where higher pressure liquid from the reservoir flows through the sandface into the wellbore. In both overbalanced and underbalanced drilling, the presence of flow through the sandface means that the walls of the borehole are *not* perfectly sealed, a tacit boundary condition assumed in elementary petroleum engineering courses. When standard inverse models (that is, math models assuming uniform initial pressure) are used to predict liquid and rock properties from limited sets of measured “time, pressure” data points, serious and unpredictable errors will arise.

Such inverse models, developed more than two decades ago during the mid-1990s, are commonly used despite numerous Halliburton and Chevron field results in Rourke et al. [1] pointing to overbalance pressures as high 2,000 psi. Again, this incorrect usage will yield incorrect predictions, leading to formation evaluation results and economic consequences that are misleading. In this research, the conventionally accepted early-time GeoTap™ model, invented by the last author for Halliburton over two decades ago, is rigorously extended to allow both general supercharge effects in overbalanced drilling as well as outflow effects in underbalanced drilling. Detailed pressure transient examples are offered for drawdown and drawdown-buildup applications, showing essential differences between the earlier and newer algorithms. Before doing so, we review overbalanced and underbalanced drilling practices for readers unfamiliar with such procedures, and also, basic Darcy flow mathematical modeling concepts.

1.2 Overbalanced and Underbalanced Drilling

What is drilling with an overbalance? In overbalanced drilling, the pressure of the drilling fluid in the borehole is kept higher than the pressure in the formation being drilled. This technique is utilized in oil and gas drilling. By utilizing this method, formation fluids like oil or gas are kept from entering the wellbore and potentially causing a blowout. Drilling mud, sometimes referred to as drilling fluid, is poured into the wellbore during overbalanced drilling at a pressure greater than the formation pressure. As a result, the mud begins to flow into the formation, forming a “filter cake” that effectively blocks formation fluids from entering the wellbore. Increased safety, shorter drilling times, and better wellbore stability are all benefits of overbalanced drilling. However, it can also result in formation damage, increased expenses since more drilling fluid is required, and environmental issues because of how much drilling mud must be disposed of. In formation testing, this added pressure characterizes wellbore and not reservoir effects. Thus, using this data will lead to inaccurate properties predictions.

How is drilling underbalanced different? An oil and gas drilling technique known as “underbalanced drilling” involves keeping the drilling fluid’s pressure lower than the formation being drilled. This method is used to boost drilling productivity and minimize formation damage. Underbalanced drilling allows reservoir fluids to flow into the wellbore by pumping drilling fluid into the wellbore at a lower pressure than the formation pressure. By lowering the pressure in the formation, this can lessen damage to the reservoir and boost oil or gas output. Reduced formation damage, higher well productivity, and enhanced wellbore stability are benefits of underbalanced drilling. However, because particular tools and methods are needed to maintain the lower pressure in the wellbore and stop the inflow of formation fluids, it can also be more difficult and expensive to put into practice than overbalanced drilling. Overall, a number of variables, such as the reservoir's geological parameters, the intended drilling result, and economic considerations, influence the decision between overbalanced and underbalanced drilling. Like overbalanced drilling, the unwanted change to true formation pressures will lead to inaccurate predictions.

1.2.1 Supercharge Determination When Drilling a Well

Again, in order to manage formation pressure and stop formation fluids (oil, gas, or water) from flowing into the wellbore, it is common practice in well drilling to “supercharge” the mud weight (density) in the wellbore. Several parameters need to be taken into account in order to calculate the supercharge required for digging a well. Based on the depth, type of rock, and other geological information, the pressure of the formation fluids can be approximated. The weight of the mud needed to balance the formation pressure and prevent wellbore influx must be determined using this information, which is crucial. The dimensions of the wellbore, the characteristics of the drilling fluid, and the drilling parameters (such as drilling rate, weight on bit, and rotary speed) can all affect the pressure applied to the formation and the amount of mud needed to maintain stability. Safety margin - to guarantee that the wellbore is stable even if unanticipated pressure fluctuations take place, a safety buffer should be added to the predicted mud weight. After accounting for the foregoing variables, the amount of mud needed to supercharge the well can be determined using mathematics or software created specifically for the task. In order to ensure wellbore stability and minimize formation fluid intrusion during drilling operations, the mud weight can then be modified as necessary.

1.2.2 What to Look for While Drilling to Discover Overbalance

The difference between the weight of the mud used in the wellbore and the formation pressure at the depth being drilled can be used to calculate the overbalance pressure when drilling a well. The density of the drilling fluid used to keep the wellbore under pressure and eliminate drilling waste is known as the mud weight. One can use the following steps to determine the overbalance pressure. Using well logs, seismic data, or other geological data, ascertain the formation pressure at the drilling depth. This can aid in *estimating* the amount of pressure the wellbore will experience as it enters the formation. Utilizing the mud weight and wellbore depth, determine the drilling fluid's hydrostatic pressure. The formula for calculating hydrostatic pressure is $\text{hydrostatic pressure} = \text{Mud weight} \times \text{depth of wellbore}$. Hydrostatic pressure is the pressure that a fluid exerts while it is at rest.

To calculate the overbalance pressure, subtract the formation pressure from the hydrostatic pressure. The well is said to be overbalanced if the hydrostatic pressure is higher than the formation pressure. The well is said to be underbalanced if the formation pressure is higher than the hydrostatic pressure. In order to avoid formation fluid ingress or blowouts, which can be risky and expensive, it is significant to note that maintaining the right overbalance pressure is essential when drilling a well. To maintain a secure and stable wellbore, the drilling crew should regularly check the wellbore pressure and modify the mud weight as necessary.

1.2.3 How to Determine the Well's Underbalance Pressure

When drilling, the technique known as "underbalance drilling" is employed to keep the pressure of the drilling fluid below that of the formation being drilled. This enhances wellbore control and can improve drilling effectiveness. One must determine the equivalent circulation density (ECD) of the drilling fluid in order to determine the underbalance pressure for drilling a well. The drilling fluid's density, or ECD, must be high enough to counteract the pressure of the target formation being drilled. The following formula is used to compute it - $\text{ECD} = \text{MW} + (\text{Pp} - \text{Ph}) \times 0.052$ 144. Here, the drilling fluid's density, measured in pounds per gallon (ppg), is MW. Also, Pp stands for pounds per square inch, or psi, formation pressure, while Ph is the drilling fluid's hydrostatic pressure inside the wellbore in psi. After determining the ECD, one can alter the drilling fluid's density to keep the pressure below that of the formation, resulting in underbalance drilling circumstances. Underbalance drilling, however, may be a challenging and potentially dangerous method that should only be used by qualified drilling professionals with the right tools and procedures.

1.2.4 Accuracy of Supercharge Calculations Used in Well Drilling

Supercharge calculations are a crucial part of drilling wells because they assist in calculating the hydraulic pressure needed to drill through different formations. The correctness of the input data, the assumptions made, and the intricacy of the wellbore geometry are some of the variables that affect how reliable these computations are. Supercharge calculations may often be trusted when carried out by qualified experts with precise information and the right software tools. The precision of these computations can be affected by the subsurface conditions' inherent fluctuation and uncertainty, though. It is crucial to obtain high-quality data from dependable sources and to carefully analyze the assumptions made in the computations in order to reduce the possibility of

errors. The geology and subsurface conditions in the wellbore location, as well as the characteristics of the drilling fluid being employed, must also be thoroughly understood.

In the end, supercharge calculations should always be used in concert with other data and analytical approaches to assure the safety and success of drilling operations, even though they can offer useful insights into drilling operations. We emphasize that, even when supercharge calculations cannot be accurately given, the range of possible values does provide error bounds on, say permeability and anisotropy, so that the methods described in this paper are useful. For recent developments related to supercharge issues, we refer the reader to Proett, Waid and Chin [2], entitled “Wireline Formation Tester Supercharge Correction Method,” United States Patent 5,644,076, and also Proett et al. [3], entitled “Methods for Measuring a Formation Supercharge Pressure,” United States Patent 7,243,537 B2.

1.3 Modeling Concepts and Approaches

In “wireline logging” and “formation testing while drilling” (or FTWD), drilling fluid invades the reservoir rock as the drill bit penetrates an unknown rock formation. This leads to mud cake deposition at the sand face where pressures are measured. Although the formation is eventually sealed from further damage, the reservoir rock adjacent close to the sand face is typically pressurized to a level more than, and often greatly exceeding, the ambient distant pore pressure. The pressure distribution is highly non-uniform near the probe and decreases into the reservoir - this spatial heterogeneity introduces math complications in formulation and algorithm development.

To circumvent essentially mathematical difficulties, one accepted practical solution has been less than ideal - simply wait until non-equilibrium pressures dissipate, a process that can consume hours and incur high rig costs. A second approach assumes that the reservoir is initially uniform in pressure, with a magnitude identical to the distant pore pressure. While this is generally not the case, it does provide solutions that may be useful when invasion is weak and only after larger wait times.

Early on, Proett and Waid [4] assumed negligible supercharge effects and provided an *ad hoc* algebraic model based on simple mass balance considerations. After limited successes, this was replaced by Proett, Chin and Chen [5], who introduced and solved the conventional zero-supercharge model in Equations 1-4 below, now the basis for Halliburton Energy Service’s GeoTap™ real-time LWD/MWD permeability prediction service and similar industry product offerings. The method provides predictions within seconds, using pressure drawdown or drawdown-buildup data.

We emphasize that the foregoing “inverse” solution for permeability, compressibility and pore pressure is obtained analytically and written in terms of complex complementary error functions. It represents an exact solution to the zero-supercharge formulation. Detailed derivations are provided in Chin et al. [6], and importantly, Fortran source code is published in the now expired 1997 patent. The algorithm also forms the basis for data compression methods used to transmit solutions to the surface during LWD/MWD operations, as discussed in Proett et al. [7].

2. Mathematical Model, Derivations and Solutions

2.1 Conventional Zero Supercharge Formulation

In overbalanced applications, drilling mud invades the reservoir, as depicted in Figure 1. The initial pressure distribution at the near-well reservoir rock is never uniform. It decreases *into* the reservoir, with the near-steady pressure satisfying a “1/r” spherical decay in isotropic media. This is the variability experienced by the formation tester. When the tester pumps, either in drawdown or drawdown-buildup mode, additional pressures are induced by transient fluid motions, e.g., in spherical or ellipsoidal zones, depending on the isotropy or anisotropy of the underlying formation. Transient anisotropic models, under zero-supercharge conditions, are derived in Chin et al. [6].

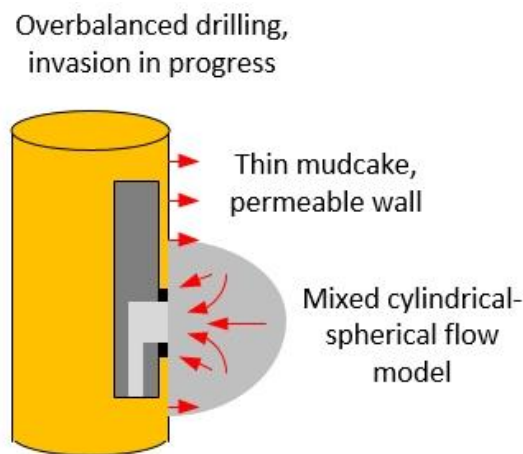


Figure 1 Overbalanced drilling with borehole influx.

Again, the “forward” zero-supercharge isotropic pressure transient solution is derived previously in Chin et al. [6] and given by Equations 1-4 below, while the complementary “inverse” algorithm and Fortran source for flow properties prediction is available in Proett, Chin and Chen [5].

$$\partial^2 P(r, t) / \partial r^2 + 2/r \partial P / \partial r = (\phi \mu c / k) \partial P / \partial t \quad (1)$$

$$P(r, t=0) = P_0 \quad (2)$$

$$P(r = \infty, t) = P_0 \quad (3)$$

$$(4\pi R_w^2 k / \mu) \partial P(R_w, t) / \partial r - VC \partial P / \partial t = Q(t) \quad (4)$$

Here, $P(r, t)$ represents the Darcy pressure at radial location “r” and time “t,” P_0 is pore pressure, R_w is nozzle effective spherical radius, V is flowline volume, and $Q(t)$ is volume pumping flow rate. Also, ϕ denotes the porosity, μ the Newtonian viscosity, c the compressibility and k is a constant isotropic permeability. Note that Equation 1 describes transient mass balance in isotropic media, while Equation 4 applies to pump piston actions. Equations 2 and 3 state that the initial pressure is spatially uniform and identical to the pore pressure in the distant farfield.

2.2 Conventional Zero Supercharge Inverse Solution

2.2.1 Transient *Isotropic* Darcy Flow - Forward Solutions - Module FT-00

Equations 1-4 describe, respectively, (1) mass conservation under transient, isotropic, compressible liquid conditions; (2) the constant initial pressure P_0 in the medium; (3) the farfield background pressure assumed equal to the initial pressure; and, (4) the mass balance boundary condition at the fluid source or sink. $P(r,t)$ represents pressure in the homogeneous porous medium; r is the spherical radius and t is time; and ϕ , μ and k are porosity, Newtonian liquid viscosity and isotropic permeability. Note that c and C are compressibilities in the medium, and second, in the formation tester flowline. Also, R_w is the spherical radius at the source, V is the flow line volume and $Q(t)$ is volume flow rate.

The above formulation employs a classical source model for spherically symmetric flows exiting or entering the needle orifice. The “ $4\pi R_w^2 k/\mu \partial P(R_w,t)/\partial r$ ” represents the contribution to $Q(t)$ due to flow through an enclosed spherical surface. This arises as the product of the fluid velocity $k/\mu \partial P/\partial r$ and the surface area $4\pi R_w^2$, while “ $VC \partial P/\partial t$ ” is associated with fluid expansion and decompression in the flow line. We next describe our exact, closed form analytical solution for the general problem.

To solve the above, we introduce the *italicized* dimensionless variables $r = r/r^*$, $t = t/t^*$, $p(r,t) = \{P(r,t) - P_0\}/p^*$ and $Q(t) = Q_0 F(t)$, and second, require $r^* = VC/(4\pi R_w^2 \phi c)$, $t^* = V^2 C^2 \mu/(16\pi^2 R_w^4 k \phi c)$ and $p^* = VCQ_0\mu/(16\pi^2 R_w^4 k \phi c)$. Here Q_0 is a positive or negative reference flow rate, and the dimensionless function $F(t)$ is given. For continuous constant flow rates, $F(t)$ is unity; for piecewise-constant multi-rate pumping, $F(t)$ can be represented by a sequence of step functions. Here we take $Q(t) = Q_0 F(t) = Q_0$ and $F(t) = 1$ for constant flow rates, with $Q_0 > 0$ for withdrawal and $Q_0 < 0$ for injection. The problem is then reduced to its simplest dimensionless form containing the sole input parameter r_w , that is $\partial^2 p(r,t)/\partial r^2 + 2/r \partial p/\partial r = \partial p/\partial t$, $p(r,0) = 0$, $p(\infty,t) = 0$ and $\partial p(r_w,t)/\partial r - \partial p/\partial t = F(t)$.

This equivalent model contains only the single dimensionless radius $r_w = 4\pi R_w^3 \phi c/(VC)$. Laplace transforms are used to develop an exact solution for $p(r,t)$. If we define *complex* constants β_1 and β_2 with $\beta_1 = +1/2 - 1/2 \sqrt{1 - 4 r_w^{-1}}$ and $\beta_2 = +1/2 + 1/2 \sqrt{1 - 4 r_w^{-1}}$, it is possible to show that the exact real dimensionless source pressure for all space and time for a constant rate $F = 1$ is $p_{exact}(r_w,t) = \{1/(\beta_1 - \beta_2)\} \{ \beta_1^{-1} - \beta_1^{-1} \exp(\beta_1^2 t) \operatorname{erfc}(\beta_1 \sqrt{t}) - \beta_2^{-1} + \beta_2^{-1} \exp(\beta_2^2 t) \operatorname{erfc}(\beta_2 \sqrt{t}) \}$.

Here, “*erfc*” denotes the “complex complementary error function” with complex arguments described in standard mathematical reference books. Returning to dimensional variables, the physical pressure becomes $P(r,t) = P_0 + p^* p(r,t)$ where P^* , r and t are defined previously. This solution can be simplified in certain limits. Taylor series expansions lead to early time solutions, while asymptotic expansions in reciprocal powers of time yield later-time solutions, so that $P(R_w,t)_{early-time} \approx P_0 - Q_0 t/(VC)$ and $P(R_w,t)_{late-time} \approx P_0 - Q_0 \mu/(4\pi R_w k) + \{Q_0 \mu/(4\pi k)\} \sqrt{\phi \mu c/(\pi k t)}$. The dimensional result for $P(R_w,t)$ at “early to intermediate times” follows from using the approximations $e^t \approx 1 + t + t^2/2! + t^3/3! + \dots$ and $\operatorname{erfc}(z) \approx 1 - 2\pi^{-1/2} \exp(-z^2) \sum 2^n z^{2n+1}/\{(1)(3) \dots (2n+1)\}$ where the sum is taken over $(0, \infty)$. Expansions in terms of rational polynomial functionals are also possible. The resulting expressions, discussed in our treatment of the inverse problem, enable straightforward solutions to complicated problems.

The above results apply to constant rate processes. In practice, it may not be possible to control pump speeds precisely and variable rates would be the result. It is also possible that sequences of

different constant rates are required to perform multiple pressure tests. “Convolution integral” approaches are described in advanced calculus text books; if the solution to a constant rate problem is available, one can construct the solution to a variable rate problem using superposition methods. In the analytical model, we assumed a constant plunger speed with a dimensionless function of $F = 1$. When $F = F(\tau)$ in general, where τ is dimensionless, the dimensionless pressure, is now

$$p_{exact}(r_w, t) = \{1/(\beta_1 - \beta_2)\} \times \int_0^t F(\tau) \{ \beta_2 \exp(\beta_2^2(t - \tau)) \operatorname{erfc} \beta_2 \sqrt{t - \tau} - \beta_1 \exp(\beta_1^2(t - \tau)) \operatorname{erfc} \beta_1 \sqrt{t - \tau} \} d\tau$$

If $F(\tau)$ takes the form of piece-wise constant rates, the solution can be expressed in closed analytical form using standard superposition methods. We will use the result for a two-rate drawdown and buildup processes in our study of applications later.

2.2.2 Transient *Isotropic and Transversely Isotropic* Single Flow Rate - Inverse Solutions - Module PTA-APP-01B

The exact pressure solutions above can be used to solve inverse problems for fluid and porous media properties. Consider the early time asymptotic solution. If discrete sets of early data were used to evaluate $P(R_w, t)$ and time t , and the results plotted with pressure on the vertical axis and time on the horizontal, the vertical intercept of the straight line gives the background pressure P_0 . The slope of the straight line measured is $-Q_0/(VC)$. Since Q_0 and V are known, the value of C follows. While P_0 is predicted as stated, it can be error prone since initial formation contacts may be erratic since the tool pad may not have anchored in place. A more precise method for P_0 is offered later.

Permeability prediction from “early to intermediate time” data is possible using the full complementary error function solutions in $P(r, t) = P_0 + p^* p(r, t)$ where P^* , and r and t were defined in terms of dimensional quantities. Again, the above derivation assumes constant rate pressure drawdown or buildup. We had noted that different series expansions for e^t and $\operatorname{erfc}(z)$ are available, for example, using exponentials and rational polynomials. Such results are conveniently obtained with algebraic manipulation software. It is possible to repeat the pressure derivation for transversely isotropic media, where the two permeabilities in the “horizontal plane” are k_h , and the permeability perpendicular to this plane is the “vertical value” k_v . When this is done, the resulting pressure function is identical, except that the isotropic k is replaced by $k_h^{2/3} k_v^{1/3}$. The leading approximations, in dimensional variables, will take the general form $P_w(t) \approx P_0 + A H(Bt)$, where $P_w(t)$ denotes the unsteady pressure at the source, $H(B)$ is a known function of B that depends on the p series expansion used, and $A = \mu Q_0 / (4\pi R_w k_h^{2/3} k_v^{1/3})$ and $B = 4\pi R_w k_h^{2/3} k_v^{1/3} / (\mu VC)$ are positive constants.

For inverse applications, we assume that $P_w(t)$ is available at three discrete sets of time values, that is, $P_{w,\#1}$ at t_1 , $P_{w,\#2}$ at t_2 and $P_{w,\#3}$ at t_3 , (the # emphasizes that these are numbers obtained from measured data). The unknown parameters to be determined are P_0 , the effective mobility $k_h^{2/3} k_v^{1/3} / \mu$ and the compressibility C . The latter two quantities are deducible from A and B whose values are in turn numerically obtained as follows. First we write our data relations as $P_{w,\#1} - P_0 \approx A H(Bt_1)$, $P_{w,\#2} - P_0 \approx A H(Bt_2)$ and $P_{w,\#3} - P_0 \approx A H(Bt_3)$ where the left sides are directly measured changes relative to background pressure. Next we divide the first equation by the second, showing that

$H(Bt_1)/H(Bt_2) \approx (P_{w,\#1} - P_0)/(P_{w,\#2} - P_0)$ where the right side value is known experimentally or from synthetic validation data.

The above equation, completely independent of A and P_0 and containing only the unknown B, represents a nonlinear equation for B expressed in terms of the function H. Importantly, $H(Bt_1)/H(Bt_2)$ is a monotonic function of B, so that B can be determined iteratively by incrementing B successively from zero until the right-side value is achieved. A half-step corrective procedure can be used to accelerate the convergence. Once B is known, the first equation $P_{w,\#1} - P_0 \approx A H(Bt_1)$ can be used to determine A since " $P_{w,\#1} - P_0$ " is known. With A and B available, the third equation can be used to predict P_0 where t_3 information is finally used. As noted, $k_h^{2/3}k_v^{1/3}/\mu$ and the compressibility C can be calculated from A and B. Thus, $k_h^{2/3}k_v^{1/3}/\mu$, C and P_0 are fully determined.

The above method, requiring three data sets of pressure and time values, utilizes data from the first few seconds of measured transients. For example, if the net time from initial nozzle contact to pressure equilibrium is fifteen seconds, data from 0, 5 and 10 sec would ensure the linear independence of the three equations used. The inverse approach above applies only to problems with single-rate pumping, whether building up or drawing down in pressure. Isotropic and transversely isotropic media are permitted and transient pressure data can be measured near the nozzle orifice. To predict properties from the second cycle of drawdown-buildup and buildup-drawdown processes, we first construct the required dimensionless pressure function by superposition. This is done by adding, to the previous function, a second similar function in which the sign of the flow rate is reversed and the time coordinate is time-shifted by the time at which the second cycle begins. A similar "three pressure data point" algorithm can be constructed, which forms the basis of the calculations presented later. This algorithm provides a better prediction to pore pressure than the simple method utilizing early time data because nozzle measurements are collected after the formation testing nozzle has fully stabilized downhole.

2.3 Supercharge Extension to Conventional Inverse Model

How can we incorporate general supercharged overbalanced and underbalanced flow effects into our solution to the inverse solution? Our approach requires us to first revise the foregoing forward formulation with a change to the initial condition in Equation 2. This is the only required modification. Thus, we consider the initial-boundary value problem defined by Equations 5-8. Once this is solved, the inverse procedure proceeds in an identical manner to that already given.

$$\partial^2 P(r, t) / \partial r^2 + 2/r \partial P / \partial r = (\phi \mu c / k) \partial P / \partial t \quad (5)$$

$$P(r, t = 0) = P_0 + Z/r, Z > 0, R > R_w \quad (6)$$

$$P(r = \infty, t) = P_0 \quad (7)$$

$$(4\pi R_w^2 k / \mu) \partial P(R_w, t) / \partial r - VC \partial P / \partial t = Q \quad (8)$$

For Equation 6, we define $Z = (P_{bh} - P_0) R_w > 0$ where P_{bh} is the drilling fluid pressure. Conventionally, the overbalance " $P_{bh} - P_0$ " is assumed in the 200-250 psi range, already a large differential. However, Halliburton and Chevron Thailand field results, as discussed in Rourke et al. [1], and further in Halliburton [8], found that overbalances exceeding 2,000 psi were common to over three hundred wells, and especially for infill drilling where the reservoir is depleting. For

problems such as these, the use of inverse models based on the conventional formulation will lead to incorrect predictions of pore pressures, permeabilities and compressibilities. However, formulations based on Equations 5 - 8 *will* provide proper physical and mathematical models for both forward and inverse problems.

Equation 6 reports what the source probe essentially measures. The symbol P_0 in Equation 7 represents as before the background pressure in the farfield of the reservoir. Our new initial condition recognizes that pressures exceed pore pressure level when the measuring tool first operates within the reservoir sand. In fact, the assumed Z/r behavior is consistent with the expected monotonic decay obtained on a local spherical flow basis. The model accounts for the high pressures that are trapped in the sand face near the formation tester nozzles until they are dissipated. This is important because overbalance effects predominate in modern lower permeability formations with thinner mud cakes. Supercharge effects always dissipate with time and lead to uniform conditions in space, but initially, they will distort the true pressures required for good formation evaluation.

Again, the only difference between the problem formulations in Equations 1 - 4 and 5 - 8 lies in the nonzero Z/r initial pressure introduced. That is, the earlier solution is now modified by a non-negligible superposed pressure field varying with Z/r dependence. While this change appears to be simple, the analysis is non-trivial given that original solutions to the zero-supercharge formulation involved complicated Laplace transform operations. However, it turns out that important simplifications are possible when the formulation is re-expressed in terms of an auxiliary pressure function whose initial pressure is uniform (as in Equation 2), but with a modified flow rate function (to that shown in Equation 4). This represents a simple algebraic transform, but importantly, exact, closed form analytical solutions are straightforwardly obtained that can be evaluated using the algorithm and source code presented in Proett, Chin and Chen [5].

3. Applications - Comparisons of Supercharge Solutions with Conventional Simplified Models

In the 1990s, validations to the zero-supercharge inverse model were exclusively obtained from lab-based measurements, which compared predicted permeabilities to those obtained from actual core samples. Since experiments, which introduce artifacts, do not provide fully accurate results, evaluation uncertainties remained. Later, Chin et al. [6] developed a simulator for “forward” problems, overcoming numerical issues arising from complex complementary error functions, solving for “pressure versus time” when input properties are given. The work was based on Equations 1-4.

The resulting “app,” known as FT-00, produced exact pressure versus time solutions in less than one second for drawdown-buildup problems, reduced the need for lab experiments. To be sure, exact synthetic pressure transient data from FT-00 could be created from prescribed fluid, rock and flowline inputs - and the same parameters could then be predicted from this data using approximate inverse models developed for real-time downhole formation evaluation. The availability of FT-00 supported job planning applications in the field, for example, estimating well logging times required in reservoirs with different permeabilities and fluid viscosities. But more importantly, it allowed developers to evaluate the accuracy of approximate inverse models designed to predict permeability, compressibility and pore pressure. *In this Section 3, we will address “pressure drawdown” applications only, followed by “drawdown-buildup” in Section 4.* This separation is made for presentation purposes.

3.1 Exercise DD-1, Drawdown Only, High Overbalance

In this research, we also modified FT-00 (using Equations 1-4) to include Z/r effects for extended simulation capabilities needed in overbalanced drilling. We used our “modified, forward FT-00” to create synthetic pressure transient streams with overbalanced pressures. This data was then interpreted, first using a conventional (incorrect) zero-supercharge model, and second, with our new inverse model fully accounting for supercharged pressure. The “pressure versus time” result of the forward simulation *with supercharge*, assuming the inputs boxed below, are shown in Figure 2.

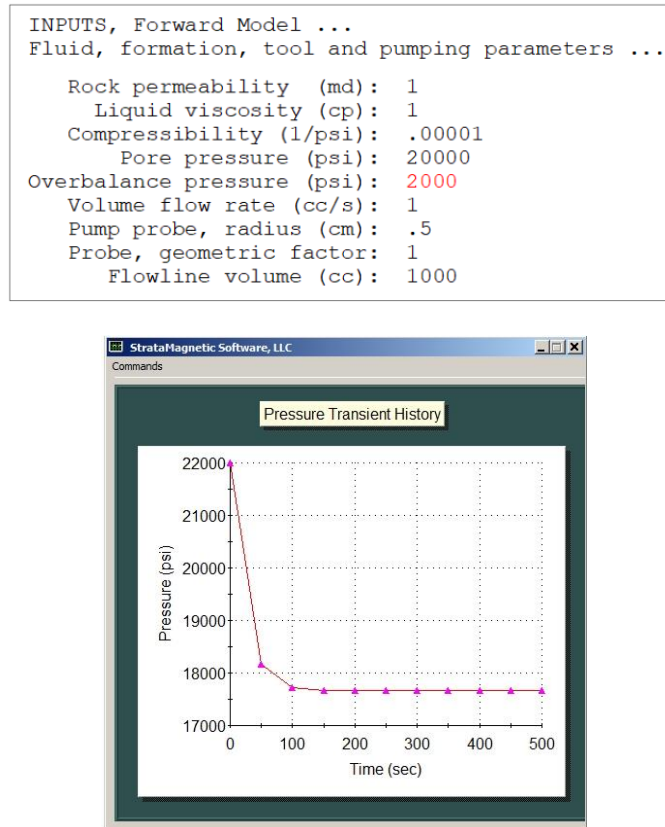


Figure 2 Transient response with overbalanced pressure.

For this first exercise, we apply the *new* inverse solver to synthetic pressures from 10, 20 and 30 sec, of 20,489 psi, 19,505 psi and 18,865 psi, and enter the 2,000 psi overbalance assumed from forward synthetic data inputs. In summary, the inverse inputs are

INPUTS, Inverse Model ...

| | |
|-----------------------------|-------|
| Volume flow rate (cc/s): | 1 |
| Pump probe, radius (cm): | .5 |
| Probe, geometric factor: | 1 |
| 1st Point Time T1 (sec): | 10 |
| Pressure P1 (psi): | 20489 |
| 2nd Point Time T2 (sec): | 20 |
| Pressure P2 (psi): | 19505 |
| 3rd Point Time T3 (sec): | 30 |
| Pressure P3 (psi): | 18865 |
| Overbalance pressure (psi): | 2000 |

Predictions are extremely good, showing a background pressure of 20,003 psi versus 20,000 psi, a 1.0164 md/cp mobility in place of 1 md/cp, plus a compressibility of $0.0100 \times (\text{cc}/\text{FloLineVol})$ per psi. Since the flowline volume is 1,000 cc, we have 0.00001 1/psi, exactly as assumed (we had used a very high test oil compressibility ten times larger than that of water, which results in slower decays). Predicted results are shown below.

```
Pore pressure and mobility predicted ..
      Pore pressure (psi):    20003.0000
Spherical mobility (md/cp):    1.0164
FloLineVol*Comp (cm^5/lbf):    0.0644
      Compressibility (1/psi):    0.0100 x (cc/FloLineVol)
```

Then the predictive calculation was repeated with an *incorrect* zero overbalance pressure input inconsistent with that used in the transient model generating the pressure data - that is, we used the conventional zero-supercharge model absent of formation invasion. The results are poor. Calculations show 22,003 psi versus 20,000 psi, 0.5463 md/cp versus 1 md/cp, and a fluid compressibility formula $0.0054 \times (\text{cc}/\text{FloLineVol})$ per psi versus $0.0100 \times (\text{cc}/\text{FloLineVol})$ per psi. These predictions are clearly unsatisfactory.

```
INPUTS, Inverse Model
      Volume flow rate (cc/s):    1
      Pump probe, radius (cm):    .5
      Probe, geometric factor:    1
      1st Point Time T1 (sec):    10
      Pressure P1 (psi):    20489
      2nd Point Time T2 (sec):    20
      Pressure P2 (psi):    19505
      3rd Point Time T3 (sec):    30
      Pressure P3 (psi):    18865
      Overbalance pressure (psi):    0

Pore pressure and mobility predicted ..
      Pore pressure (psi):    22003.0000
Spherical mobility (md/cp):    0.5463
FloLineVol*Comp (cm^5/lbf):    0.0346
      Compressibility (1/psi):    0.0054 x (cc/FloLineVol)
```

3.2 Exercise DD-2, Drawdown Only, High Overbalance

Here, the forward model is identical to that assumed above but with a tenfold smaller mobility. The supercharged pressure transient response is shown in Figure 3. Our first inverse calculation used three arbitrary points, namely 10 sec, 20,937 psi, 20 sec, 19,919 psi, and 30 sec, 18,944 psi, and the 2,000 psi excess pressure. Predictions are good, showing a 20,000 psi pore pressure, a 0.1040 md/cp versus 0.1 md/cp mobility, and a compressibility formula of $0.0100 \times (\text{cc}/\text{FloLineVol})$ per psi agreeing with the forward model.

```

INPUTS, Forward Model ...
Fluid, formation, tool and pumping parameters ...

Rock permeability (md): 0.1
Liquid viscosity (cp): 1
Compressibility (1/psi): .00001
Pore pressure (psi): 20000
Overbalance pressure (psi): 2000
Volume flow rate (cc/s): 1
Pump probe, radius (cm): .5
Probe, geometric factor: 1
Flowline volume (cc): 1000
Plot every "NSEC" seconds: 50
    
```

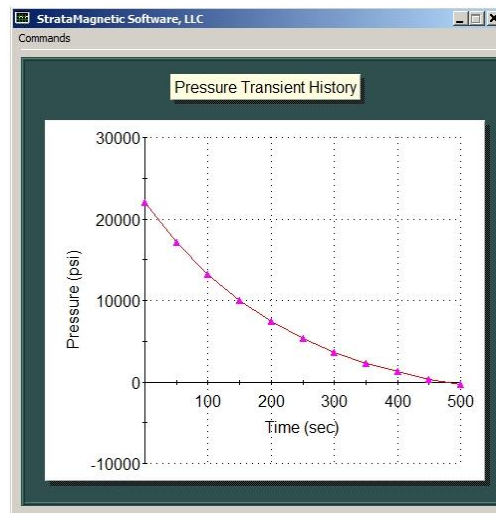


Figure 3 Pressure response with overbalance assumption.

```

INPUTS, Forward Model ...
Fluid, formation, tool and pumping parameters ...

Formation permeability ..... (md): 0.1000E+00
Viscosity ..... (cp): 0.1000E+01
Liquid compressibility ..... (1/psi): 0.1000E-04
Pore pressure ..... (psi): 0.2000E+05
Overbalance pressure ..... (psi): 0.2000E+04
Volume flow rate ..... (cc/s): 0.1000E+01
Probe radius ..... (cm): 0.5000E+00
Geometric factor ..... (dimensionless): 0.1000E+01
Effective radius ..... (cm): 0.5000E+00
Flowline volume ..... (cc): 0.1000E+04
    
```

In the second inverse calculation, we use the incorrect conventional older inverse model assuming zero-supercharge. The mobility is 0.0956 md/cp while the compressibility value is “0.0092.” These compare well with the exact input values of 0.1 md/cp and “0.01.” However, an incorrect pore pressure of 22,000 psi is obtained instead of 20,000 psi.

3.3 Exercise DD-3, High Overbalance

For the synthetic data in this inverse calculation, we assumed a higher mobility of 10 md/cp relative to our prior exercises. That is, we assumed the pressure transient response in Figure 4.

```

INPUTS, Forward Model ...
Fluid, formation, tool and pumping parameters ...

Rock permeability (md): 10
Liquid viscosity (cp): 1
Compressibility (1/psi): .00001
Pore pressure (psi): 20000
Overbalance pressure (psi): 2000
Volume flow rate (cc/s): 1
Pump probe, radius (cm): .5
Probe, geometric factor: 1
Flowline volume (cc): 1000
Plot every "NSEC" seconds: 1

```

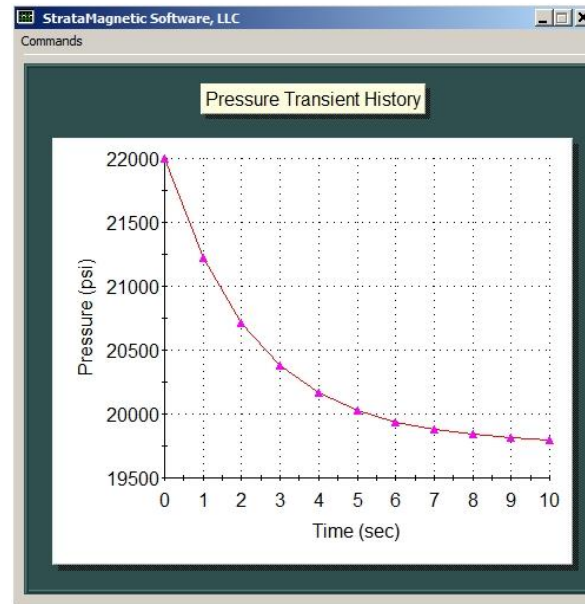


Figure 4 Transient response with overbalanced pressure.

The time versus pressure data here were 5 sec, 20,028 psi, 10 sec, 19,797 psi, and 20 sec, 19,767 psi. For our initial inverse analysis, we assumed the known 2,000 psi overbalance pressure, and predicted 20,014 psi, 9.5467 md/cp and “0.0094” for compressibility. These values compare favorably 20,000 psi, 10 md/cp and “0.01” assumed for the synthetic forward data. In the second inverse calculation, the conventional zero-supercharge inverse model was used and the results were not good. For pore pressure, we found 22,014 psi versus 20,000 psi. Also, the mobility determined was 1.0512 md/cp compared with a known 10 md/cp - a ten-fold ten discrepancy, although the compressibility was obtained correctly.

3.4 Exercise DD-4, Drawdown Only, Qualitative Pressure Trends

Before pursuing inverse studies, it is useful to qualitatively understand overbalance effects. The new forward model automatically plots pressure versus time responses for different overbalances. For example, in the input summary below, the red “200 psi trigger” creates pressure transients for overbalance levels of 0, 200, 400, 600 and 800 psi. From computed results, note that the initial $t = 0$ pressure contains the effects of high pressure overbalance, but that all pressure level responses correctly diffuse to the same pressure at large times. The results also show that relevant time scale is approximately 240 sec with pressures of 17,668 psi. From Figure 5, we observe that as overbalance effects disappear with time, all line graphs grow closer and closer. The convergence

rate depends on tool, fluid and formation parameters. The effect of overbalance is *not* the commonly assumed simple shift of the static responses with “no overbalance.” It is important to note that the time required for overbalance effects to completely dissipate is also a product of the software models developed here.

```

INPUTS, Forward Model ...
Fluid, formation, tool and pumping parameters ...

Rock permeability (md): 1
Liquid viscosity (cp): 1
Compressibility (1/psi): .00001
Pore pressure (psi): 20000
Overbalance pressure (psi): 200
Volume flow rate (cc/s): 1
Pump probe, radius (cm): .5
Probe, geometric factor: 1
Flowline volume (cc): 1000
Plot every "NSEC" seconds: 5
    
```

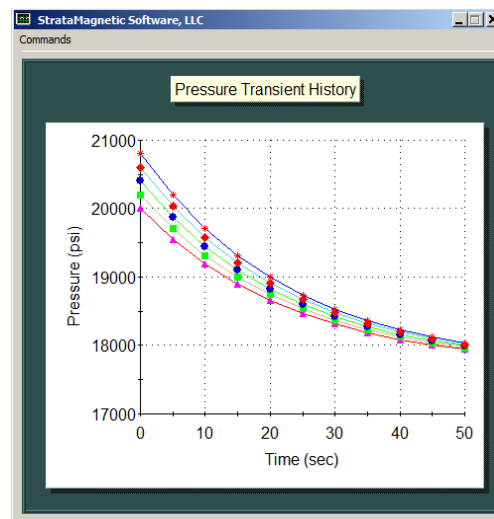


Figure 5 Pressure versus time for different overbalance pressures.

In applications with higher overbalance pressures, supercharge effects may not diffuse until about an hour, but it is possible to greatly exceed this depending on the rock permeability levels assumed. Operationally, it is not advisable to simply wait for complete dissipation, since this increases the risk of stuck tools and contributes rig time usage. When overbalance pressure estimates are available, it is desirable to use improved inverse models accounting for supercharge.

3.5 Exercise DD-5, Drawdown Only, Pressure Diffusion Trends

Additional calculated results assuming a broader range of overbalances are shown in Figure 6 without further comment. Note that a high 10 md permeability is assumed and supercharge effects dissipate very quickly. Figure 5 and Figure 6 demonstrate the physically expected fact that lowering background rock permeability values will increase the time needed to achieve pressure equilibrium. We emphasize that the time scale for this diffusion process is completely predictable and fully determined using the model in Equations 5-8.

```

FORMATION TESTER, FORWARD PRESSURE TRANSIENT MODEL
Forward pressure transient predictions for drawdown-only
applications, for low mobility, isotropic, supercharged
flows where flowline storage is not negligible.

Fluid, formation, tool and pumping parameters ...

Formation permeability ..... (md):    0.1000E+02
Viscosity ..... (cp):    0.1000E+01
Liquid compressibility ..... (1/psi):    0.1000E-04
Pore pressure ..... (psi):    0.2000E+05
Overbalance pressure ..... (psi):    0.1000E+04
Volume flow rate ..... (cc/s):    0.1000E+01
Probe radius ..... (cm):    0.5000E+00
Geometric factor ..... (dimensionless):    0.1000E+01
Effective radius ..... (cm):    0.5000E+00
Flowline volume ..... (cc):    0.1000E+04
    
```

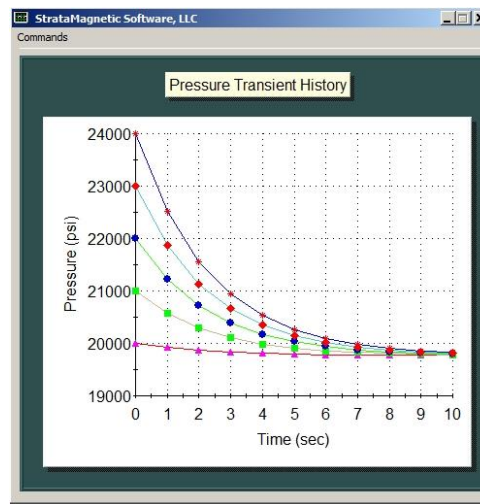


Figure 6 Transients results for selected overbalance pressures.

4. Applications - Drawdown/Buildup

4.1 Exercise DDBU-1 - Drawdown-Buildup, High Overbalance

We turn to drawdown-buildup problems. The dual-rate supercharge model uses data from the buildup (as opposed to the drawdown) part of the pressure curve for inverse calculations. The forward model assumes a 2,000 psi overbalance, the mobility is 10 md/cp, while the time at which the formation tester piston stops fluid retracting is 5 sec. In the pressure versus time curve, shown in Figure 7, the expected buildup is not quite building up. In fact, the response is almost flat due to the effects of mud supercharge. This calculated effect is real.

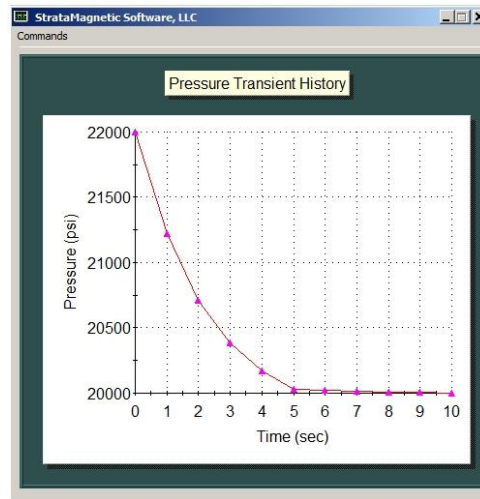


Figure 7 Pressure versus time with high overbalance.

In fact, rapid drawdowns followed by a level “buildups” always suggests strong overbalance effects requiring supercharge inverse models. Now we describe inverse results. The (time, pressure) data points were selected at 5, 8 and 15 sec, with 20,028 psi, 20,008 psi and 20,000 psi, respectively. In the *first* inverse exercise using the supercharge procedure, we assume a 2,000 psi overbalance, and the predictions of 19,999 psi, 8.609 md/cp and “0.0090” for compressibility are good relative to 20,000 psi, 10 md/cp and “0.01.” In the *second* exercise, we assume a zero overbalance (as in the conventional approach) without supercharge. The background pressure is correctly predicted at 19,999 psi when compared with 20,000 psi, but the mobility of -71.849 md/cp is negative as is the compressibility. These values are, of course, not acceptable.

```

INPUTS, Forward Model ...
Fluid, formation, tool and pumping parameters ...

Rock permeability (md): 10
Liquid viscosity (cp): 1
Compressibility (1/psi): .00001
Pore pressure (psi): 20000
Overbalance pressure (psi): 2000
Volume flow rate (cc/s): 1
Pump probe, radius (cm): .5
Probe, geometric factor: 1
Flowline volume (cc): 1000
Time drawdown ends (sec): 5
    
```

Inverse Calculation 1 (with supercharge)

INPUTS, Inverse Model ...

```

Volume flow rate (cc/s):      1
Pump probe, radius (cm):      .5
Probe, geometric factor:      1
  Stop time TDD1 (sec):      5
1st Point Time T1 (sec):      5
  Pressure P1 (psi):          20028
2nd Point Time T2 (sec):      8
  Pressure P2 (psi):          20008
3rd Point Time T3 (sec):      15
  Pressure P3 (psi):          20000
Overbalance (psi):            2000
    
```

Pore pressure and mobility predicted .. Excellent results below
from supercharge model!

```

Pore pressure (psi):      19999.000
Spherical mobility (md/cp): 8.609
FloLineVol*Comp (cm^5/lbf): 0.0583
Compressibility (1/psi):  0.0090 x (cc/FloLineVol)
    
```

Inverse Calculation 2 (no supercharge)

INPUTS, Inverse Model ...

```

Volume flow rate (cc/s):      1
Pump probe, radius (cm):      .5
Probe, geometric factor:      1
  Stop time TDD1 (sec):      5
1st Point Time T1 (sec):      5
  Pressure P1 (psi):          20028
2nd Point Time T2 (sec):      8
  Pressure P2 (psi):          20008
3rd Point Time T3 (sec):      15
  Pressure P3 (psi):          20000
Overbalance (psi):            0
    
```

Pore pressure and mobility predicted ... Poor results below for
zero-supercharge assumption!

```

Pore pressure (psi):      19999.000
Spherical mobility (md/cp): -71.849
FloLineVol*Comp (cm^5/lbf): -0.4866
Compressibility (1/psi):  -0.0754 x (cc/FloLineVol)
    
```

4.2 Exercise DDBU-2, Drawdown-Buildup, High Overbalance

In this example, we will change DDBU-1 forward model inputs, to emphasize the buildup part of the pressure versus time curve - the curve now displays pressure increasing in time as in Figure 8. The data points used for the inverse calculations are 5 sec, 19,823 psi, 10 sec, 19,979 psi, and 19 sec, 20,000 psi.

INPUTS, Forward Model ...

Fluid, formation, tool and pumping parameters ...

```

Rock permeability (md):      10
Liquid viscosity (cp):      1
Compressibility (1/psi):     .00001
Pore pressure (psi):          20000
Overbalance pressure (psi):   2000
Volume flow rate (cc/s):     2
Pump probe, radius (cm):     .5
Probe, geometric factor:     1
Flowline volume (cc):        1000
Time drawdown ends (sec):    5
    
```

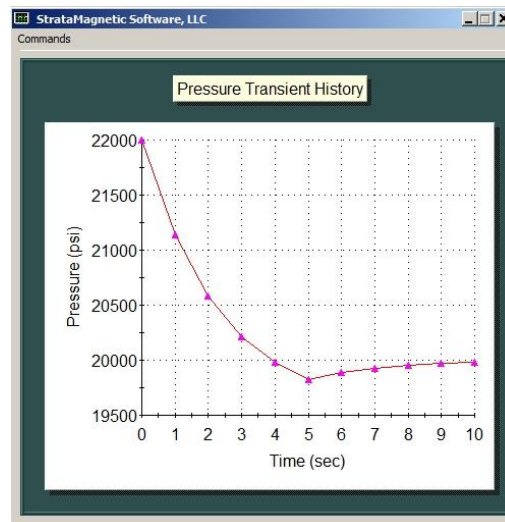


Figure 8 Pressure versus time with overbalance.

| Inverse Calculation 1 | |
|-----------------------------------------|----------------------------------------------|
| INPUTS, Inverse Model ... | |
| Volume flow rate (cc/s): | 2 |
| Pump probe, radius (cm): | .5 |
| Probe, geometric factor: | 1 |
| Stop time TDD1 (sec): | 5 |
| 1st Point Time T1 (sec): | 5 |
| Pressure P1 (psi): | 19823 |
| 2nd Point Time T2 (sec): | 10 |
| Pressure P2 (psi): | 19979 |
| 3rd Point Time T3 (sec): | 19 |
| Pressure P3 (psi): | 20000 |
| Overbalance (psi): | 2000 . . . Correct overbalance pressure used |
| Pore pressure and mobility predicted .. | |
| Pore pressure (psi): | 20000.000 |
| Spherical mobility (md/cp): | 9.901 |
| FloLineVol*Comp (cm^5/lbf): | 0.0640 |
| Compressibility (1/psi): | 0.0099 x (cc/FloLineVol) |

The above predictions are very good, with a 20,000 psi pore pressure as assumed, and a mobility of 9.901 md/cp compared with 10 md/cp, and a compressibility of “0.0099” versus “0.01.” The above calculation assumed a 2,000 psi overbalance. In the subsequent exercise, a vanishing value is used to mimic the conventional inverse model not accounting for invasion. In this calculation, the pore pressure is accurate, but the mobility is 23.403 md/cp compared with a correct 10 md/cp. The compressibility is “0.0235” is twice that of the assumed “0.01.”

```

Inverse Calculation 2

INPUTS, Inverse Model ...

Volume flow rate (cc/s):      2
Pump probe, radius (cm):      .5
Probe, geometric factor:      1
Stop time TDD1 (sec):        5
1st Point Time T1 (sec):      5
    Pressure P1 (psi):        19823
2nd Point Time T2 (sec):      10
    Pressure P2 (psi):        19979
3rd Point Time T3 (sec):      19
    Pressure P3 (psi):        20000
Overbalance (psi):            0
Pore pressure and mobility predicted ..

    Pore pressure (psi):      20000.000
Spherical mobility (md/cp):    23.403
FloLineVol*Comp (cm^5/lbf):    0.1513
Compressibility (1/psi):       0.0235 x (cc/FloLineVol)
    
```

4.3 Exercise DDBU-3, Drawdown-Buildup, High Overbalance

For the present calculation, the “buildup curve” decreases with time, as shown in Figure 9. This part of the transient response actually represents the pressure behavior when the formation tester piston has ceased withdrawing fluid. The time decrease results from high overbalance pressures.

```

INPUTS, Forward Model ...
Fluid, formation, tool and pumping parameters ...

Rock permeability (md):      1
Liquid viscosity (cp):      1
Compressibility (1/psi):    .00001
Pore pressure (psi):        20000
Overbalance pressure (psi):  2000
Volume flow rate (cc/s):    2
Pump probe, radius (cm):    .5
Probe, geometric factor:    1
Flowline volume (cc):       1000
Time drawdown ends (sec):   5
    
```

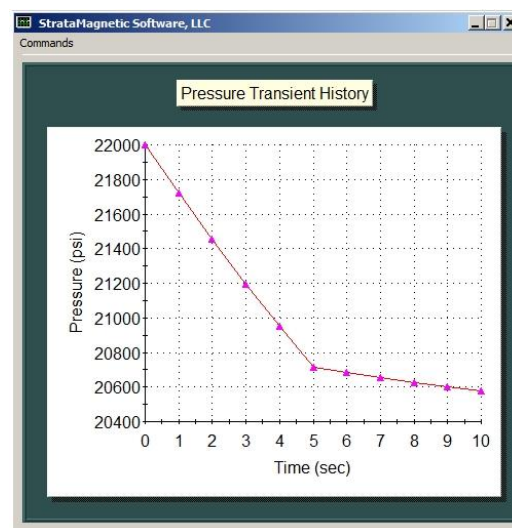


Figure 9 Pressure transient “buildup” with high overbalance.

For our (time, pressure) inverse procedure inputs, the values 5 sec, 20,714 psi, 10 sec, 20,576 psi, and 20 sec, 20,375 psi were selected. For a first inverse calculation, we assumed the 2,000 psi

overbalance. The predictions are extremely good, showing a pore pressure of 20,002 psi versus 20,000 psi, a mobility of 1.017 md/cp versus 1 md/cp, and the compressibility taking on “0.01” exactly as inputted. In the second calculation, the pore pressure is accurate, but both the mobility and compressibility are negative.

```

Inverse Calculation 1
INPUTS, Inverse Model ...

Volume flow rate (cc/s):      2
Pump probe, radius (cm):     .5
Probe, geometric factor:      1
Stop time TDD1 (sec):        5
1st Point Time T1 (sec):      5
    Pressure P1 (psi):        20714
2nd Point Time T2 (sec):      10
    Pressure P2 (psi):        20576
3rd Point Time T3 (sec):      20
    Pressure P3 (psi):        20375
Overbalance (psi):            2000

Pore pressure and mobility predicted ... Excellent results!

Pore pressure (psi):          20002.000
Spherical mobility (md/cp):    1.017
FloLineVol*Comp (cm^5/lbf):   0.0645
Compressibility (1/psi):       0.0100 x (cc/FloLineVol)
    
```

```

Inverse Calculation 2
INPUTS, Inverse Model ...

Volume flow rate (cc/s):      2
Pump probe, radius (cm):     .5
Probe, geometric factor:      1
Stop time TDD1 (sec):        5
1st Point Time T1 (sec):      5
    Pressure P1 (psi):        20714
2nd Point Time T2 (sec):      10
    Pressure P2 (psi):        20576
3rd Point Time T3 (sec):      20
    Pressure P3 (psi):        20375
Overbalance (psi):            0

Pore pressure and mobility predicted ..

Pore pressure (psi):          20002.000 ... Negative results below!
Spherical mobility (md/cp):    -1.287
FloLineVol*Comp (cm^5/lbf):   -0.0815
Compressibility (1/psi):       -0.0126 x (cc/FloLineVol)
    
```

4.4 Exercise DDBU-4, Drawdown-Buildup, 1 md/cp Calculations

From the synthetic forward data, we choose pressures at times $t = 21, 30$ and 40 sec, namely 8,815 psi, 9,194 psi and 9,475 psi, for inverse procedure (the “21 sec” occurs just after 20 sec, when piston retraction ends). The selected buildup points are taken from the rapidly varying part of the pressure transient response in Figure 10.

```

INPUTS, Forward Model ...
Fluid, formation, tool and pumping parameters ...

Rock permeability (md):      1
Liquid viscosity (cp):       1
Compressibility (1/psi):     .00001
Pore pressure (psi):         10000
Overbalance pressure (psi):  250
Volume flow rate (cc/s):     1
Pump probe, radius (cm):     .5
Probe, geometric factor:     1
Flowline volume (cc):        1000
Time drawdown ends (sec):    20
    
```

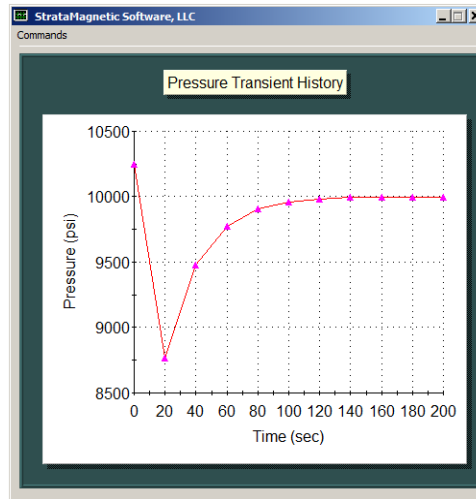


Figure 10 Pressure versus time with moderate overbalance.

We attempt to recover the inputs used in creating the synthetic transient pressure data, again using only three points “($t_1, P_{w, \#1}$), ($t_2, P_{w, \#2}$) and ($t_3, P_{w, \#3}$),” plus nozzle geometry, pump rate and overbalance pressure inputs.

```

INPUTS, Inverse Model ...

Volume flow rate (cc/s):      1
Pump probe, radius (cm):     .5
Probe, geometric factor:     1
Stop time TDD1 (sec):       20
1st Point Time T1 (sec):     21
    Pressure P1 (psi):       8815
2nd Point Time T2 (sec):     30
    Pressure P2 (psi):       9194
3rd Point Time T3 (sec):     40
    Pressure P3 (psi):       9475
Overbalance (psi):           250

Pore pressure and mobility predicted ..

Pore pressure (psi):         10000.000
Spherical mobility (md/cp):  1.011
FloLineVol*Comp (cm^5/lbf):  0.0645
Compressibility (1/psi):     0.0100 x (cc/FloLineVol)
  
```

The pore pressure of 10,000 psi is correct, while the mobility of 1.011 md/cp shows a minor 1% error. We emphasize that the inverse solver does *not* request the flowline volume V as an input - it predicts the product VC where C is compressibility. We had assumed (in the forward analysis) that $V = 1,000$ cc. The “cc/FloLineVol” term is thus 1/1,000. Multiplying 0.0100 by 1/1,000 gives 0.00001/psi, the correct assumed value. Note that the methodology devised here applies to all manufacturers’ formation testers. If the flowline volume V is available, fluid compressibility C is available from the inverse model.

4.5 Exercise DDBU-5, Drawdown-Buildup, 0.1 md/cp Calculations

In Exercise DDBU-4, the forward analysis assumed a 1 md permeability for a mobility of 1 md/cp and a moderate overbalance of 250 psi. In this exercise, we consider a tighter formation with a 0.1 md/cp mobility and an overbalance pressure of 1,000 psi.

```

INPUTS, Forward Model ...
Fluid, formation, tool and pumping parameters ...

Rock permeability (md): 0.1
Liquid viscosity (cp): 1
Compressibility (1/psi): .000003
Pore pressure (psi): 20000
Overbalance pressure (psi): 1000
Volume flow rate (cc/s): 1
Pump probe, radius (cm): .5
Probe, geometric factor: 1
Flowline volume (cc): 1000
Time drawdown ends (sec): 20
    
```

The dynamically significant part of the pressure versus time curve appears in Figure 11. The following “time, pressure” data points were used in inverse calculations, 21 sec, 15,025 psi, 30 sec, 15,625 psi, 40 sec, 16,208 psi, and 60 sec 17,151 psi.

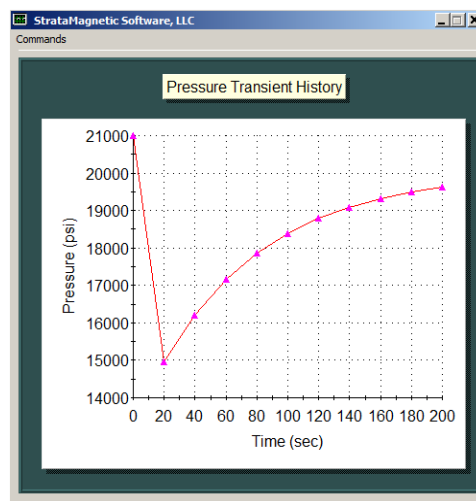


Figure 11 Pressure versus time with moderate overbalance.

For the first inverse calculation, we used pressures from times 21, 30 and 40 sec (piston motions ceased at 20 sec). Predicted mobility and compressibility are very good, but pore pressure exceeds the inputted value by 26 psi. For the second calculation, we use 21, 40 and 60 sec data. This was selected to provide a wider dynamic range for increased accuracy, as the rock considered was low in permeability. Mobility and compressibility are extremely good - the value of pore pressure, now at 19,997 psi, is close to the input value of 20,000 psi.

Inverse Calculation 1

INPUTS, Inverse Model ...

| | |
|--------------------------|-------|
| Volume flow rate (cc/s): | 1 |
| Pump probe, radius (cm): | .5 |
| Probe, geometric factor: | 1 |
| Stop time TDD1 (sec): | 20 |
| 1st Point Time T1 (sec): | 21 |
| Pressure P1 (psi): | 15025 |
| 2nd Point Time T2 (sec): | 30 |
| Pressure P2 (psi): | 15625 |
| 3rd Point Time T3 (sec): | 40 |
| Pressure P3 (psi): | 16208 |
| Overbalance (psi): | 1000 |

Pore pressure and mobility predicted ..

| | |
|-----------------------------------------|--------------------------|
| Pore pressure (psi): | 20026.000 |
| Spherical mobility (md/cp): | 0.100 |
| FloLineVol*Comp (cm ⁵ /lbf): | 0.0193 |
| Compressibility (1/psi): | 0.0030 x (cc/FloLineVol) |

Inverse Calculation 2

INPUTS, Inverse Model ...

| | |
|--------------------------|-------|
| Volume flow rate (cc/s): | 1 |
| Pump probe, radius (cm): | .5 |
| Probe, geometric factor: | 1 |
| Stop time TDD1 (sec): | 20 |
| 1st Point Time T1 (sec): | 21 |
| Pressure P1 (psi): | 15025 |
| 2nd Point Time T2 (sec): | 40 |
| Pressure P2 (psi): | 16208 |
| 3rd Point Time T3 (sec): | 60 |
| Pressure P3 (psi): | 17151 |
| Overbalance (psi): | 1000 |

Pore pressure and mobility predicted ..

| | |
|-----------------------------------------|--------------------------|
| Pore pressure (psi): | 19997.000 |
| Spherical mobility (md/cp): | 0.101 |
| FloLineVol*Comp (cm ⁵ /lbf): | 0.0194 |
| Compressibility (1/psi): | 0.0030 x (cc/FloLineVol) |

5. Concluding Remarks

It has been two decades since the commercial use of “early time, tight zone, flowline volume dependent” methods for permeability, compressibility and pore pressure in single-probe formation testing. However, as Rourke et al. [1] and Halliburton [8] importantly note, high overbalance pressures and supercharge can render conventional interpretation methods of limited value and lead to incorrect properties predictions. The new inverse model introduced here introduces an important modification to the initial pressure distribution associated with supercharge which extends the applicability of the conventional models such as GeoTap™ and similar industry methods. Only minor mathematical or programming changes are needed to upgrade tool or desktop software applications.

We emphasize that the model in this paper was derived for isotropic media, whereas in reality, formations are typically transversely isotropic. This is not a practical concern. As Chin et al. [6] show in a much more detailed derivation, the present results apply rigorously so long as “k” is regarded as an effective permeability with the value $kh^{2/3}kv^{1/3}$. Again, in field activities, there may be situations when exact overbalance pressures cannot be determined and only estimates are available (we have summarized earlier how estimates can be given). In such cases, the resulting predictions can be used to provide error bounds, useful in formation evaluation and project cost estimation, in addition to predicted values of permeabilities, compressibilities and pore pressures.

Author Contributions

X.Q. and Y.F. were responsible for project development, and L.W., Z.T. and Y.Z. performed the calculations. W.C. formulated and solved the math models, and wrote the English manuscript.

Competing Interests

The authors have declared that no competing interests exist.

References

1. Rourke M, Powell B, Platt C, Hall K, Gardner A. A new hostile environment wireline formation testing tool: A case study from the gulf of Thailand. Paper presented at the SPWLA 47th Annual Logging Symposium; 2006 June 4-7; Veracruz, Mexico. Richardson, TX: OnePetro.
2. Proett MA, Waid MC, Chin WC. Wireline formation tester supercharge correction method. Houston, Texas, USA: Halliburton Energy Services Inc; 1997; United States Patent 5,644,076.
3. Proett MA, Chin WCL, Beique JM, Hardin Jr JR, Fogal JM, Welshans D, et al. Methods for measuring a formation supercharge pressure. Houston, Texas, USA: Halliburton Energy Services Inc; 2007; United States patent US 7,243,537.
4. Proett MA, Waid MC. Wireline formation testing for low permeability formations utilizing pressure transients. Houston, Texas, USA: Halliburton Co; 1997; United States patent US 5,602,334.
5. Proett MA, Chin WC, Chen CC. Method of formation testing. 1997; United States Patent 5,703,286.
6. Chin W, Zhou Y, Feng Y, Yu Q, Zhao L. Formation testing: Pressure transient and contamination analysis. Hoboken, New Jersey: John Wiley & Sons; 2014.
7. Proett MA, Weintraub PN, Golla CA, Simeonov SD. Formation testing while drilling data compression. Houston, Texas, USA: Halliburton Energy Services Inc; 2005; United States patent US 6,932,167.
8. Halliburton staff. Testing the tight gas reservoir: Hostile-environment wireline formation tester reduces NPT in HPHT boreholes, Halliburton Energy Services Internet publication, 2018. Available from: <https://www.halliburton.com/>.